Single-shot terahertz spectroscopy using pulse-front tilting of an ultra-short probe pulse

Yoichi Kawada,* Takashi Yasuda, Atsushi Nakanishi, Koichiro Akiyama, and Hironori Takahashi

Central Research Laboratory, Hamamatsu Photonics K. K., 5000 Hirakuchi, Hamakita-ku, Hamamatsu City, Shizuoka 434-8601, Japan
**kawada401@crl.hpk.co.jp*

Abstract: We developed a single-shot terahertz pulse measurement technique using pulse-front tilting of an ultra-short probe pulse and demonstrated single-shot terahertz spectroscopy. A transmission grating was used to introduce a sufficiently large pulse-front tilt angle. A measuring time range of 23.8 ps was achieved. The measured temporal waveforms were corrected in consideration of the nonlinearity arising from the crossed-Nicols arrangement employed and the beam profiles of the probe and terahertz pulses. The characteristic spectrum of lactose was measured with a single terahertz pulse, and the effectiveness of our single-shot technique was confirmed by comparison with a conventional sampling method.

OCIS codes: (300.6495) Spectroscopy, terahertz; (320.7150) Ultrafast spectroscopy.

References and links

1. C. A. Schmuttenmaer, "Exploring dynamics in the far-infrared with terahertz spectroscopy," Chem. Rev. **104**(4), 1759–1780 (2004).
2. Z. Jiang, and X.-C. Zhang, "Electro-optic measurement of THz field pulses with a chirped optical beam," Appl. Phys. Lett. **72**(16), 1945–1947 (1998).
3. Z. Jiang, F. G. Sun, and X.-C. Zhang, "Terahertz pulse measurement with an optical streak camera," Opt. Lett. **24**(17), 1245–1247 (1999).
4. J. Shan, A. S. Weling, E. Knoesel, L. Bartels, M. Bonn, A. Nahata, G. A. Reider, and T. F. Heinz, "Single-shot measurement of terahertz electromagnetic pulses by use of electro-optic sampling," Opt. Lett. **25**(6), 426–428 (2000).
5. T. Yasui, K. Sawanaka, A. Ihara, E. Abraham, M. Hashimoto, and T. Araki, "Real-time terahertz color scanner for moving objects," Opt. Express **16**(2), 1208–1221 (2008).
6. K. Y. Kim, B. Yellampalle, A. J. Taylor, G. Rodriguez, and J. H. Glownia, "Single-shot terahertz pulse characterization via two-dimensional electro-optic imaging with dual echelons," Opt. Lett. **32**(14), 1968–1970 (2007).
7. S. P. Jamison, J. Shen, A. M. MacLeod, W. A. Gillespie, and D. A. Jaroszynski, "High-temporal-resolution, single-shot characterization of terahertz pulses," Opt. Lett. **28**(18), 1710–1712 (2003).
8. Y. Kawada, T. Yasuda, H. Takahashi, and S. Aoshima, "Real-time measurement of temporal waveforms of a terahertz pulse using a probe pulse with a tilted pulse front," Opt. Lett. **33**(2), 180–182 (2008).
9. J. Hebling, G. Almasi, I. Kozma, and J. Kuhl, "Velocity matching by pulse front tilting for large area THz-pulse generation," Opt. Express **10**(21), 1161–1166 (2002).
10. R. Wyatt, and E. E. Marinero, "Versatile single-shot background-free pulse duration measurement technique, for pulses of subnanosecond to picoseconds duration," Appl. Phys. (Berl.) **25**(3), 297–301 (1981).
11. T. Yasuda, Y. Kawada, H. Toyoda, and H. Takahashi, "Terahertz movie of internal transmission imaging," Opt. Express **15**(23), 15583–15588 (2007).
12. Zs. Bor, and B. Racz, "Group velocity dispersion in prisms and its application to pulse compression and travelling-wave excitation," Opt. Commun. **54**(3), 165–170 (1985).
13. Z. Jiang, F. G. Sun, Q. Chen, and X.-C. Zhang, "Electro-optic sampling near zero optical transmission point," Appl. Phys. Lett. **74**(9), 1191–1193 (1999).
14. Z. Jiang, X. G. Xu, and X.-C. Zhang, "Improvement of terahertz imaging with a dynamic subtraction technique," Appl. Opt. **39**(17), 2982–2987 (2000).
15. F. Miyamaru, T. Yonera, M. Tani, and M. Hangyo, "Terahertz two-dimensional electrooptic sampling using high speed complementary metal-oxide semiconductor camera," Jpn. J. Appl. Phys. **43**(No. 4A), L489–L491 (2004).
16. A. Yariv, *Optical Electronics*, 4th ed. (Wiley, 1991), p. 699.
17. M. Usami, T. Iwamoto, R. Fukasawa, M. Tani, M. Watanabe, and K. Sakai, "Development of a THz spectroscopic imaging system," Phys. Med. Biol. **47**(21), 3749–3753 (2002).

#144043 - $15.00 USD Received 11 Mar 2011; revised 25 Apr 2011; accepted 25 Apr 2011; published 25 May 2011

18. Q. Chen, M. Tani, Z. Jiang, and X.-C. Zhang, "Electro-optic transceivers for terahertz-wave applications," J. Opt. Soc. Am. B **18**(6), 823–831 (2001).
19. A. Nahata, A. S. Weling, and T. F. Heinz, "A wideband coherent terahertz spectroscopy system using optical rectification and electro-optic sampling," Appl. Phys. Lett. **69**(16), 2321–2323 (1996).

1. Introduction

A terahertz (THz) pulse generated from a femtosecond laser pulse is suitable for observing ultra-fast phenomena because of its extremely short pulse duration. This technique has been used for time-resolved measurement of a relaxation process in a semiconductor and transient conductivity in a molecular crystal [1]. This approach, however, has some drawbacks. Because femtosecond probe pulses are used to probe the THz pulses point-by-point in the conventional sampling method with lock-in detection, the result is a time-averaged temporal waveform obtained during the measurement process, and the conventional sampling method can only measure objects exhibiting phenomena that are synchronized with the repetition frequency of the laser pulses.

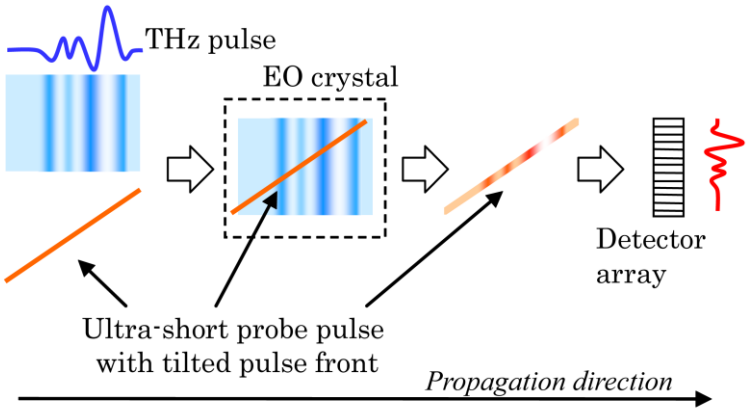

Fig. 1. Schematic representation of principle of single-shot THz waveform measurement using pulse-front tilting: Top view.

To take full advantage of the extremely short THz pulses, that is, to obtain information about the sample contained in each THz pulse, a single-shot technique for measuring the THz temporal waveform is needed. In principle, a single-shot measurement can measure the transient properties of irreversible phenomena. Some single-shot measurement methods have been proposed and demonstrated [2–8], including one that we developed using pulse-front tilting of a probe laser pulse [8]. The pulse front is the plane containing the maximum laser pulse intensity. Pulse-front tilting occurs when the laser pulse passes through dispersing elements, such as prisms or gratings. Pulse front tilting has been used to generate intense THz pulses by optical rectification in lithium niobate [9] and for autocorrelation measurement of short laser pulses [10].

Figure 1 shows the principle of our single-shot technique. A THz pulse and an ultra-short probe pulse with a tilted pulse front are collinearly and simultaneously incident on an electro-optic (EO) crystal. The ultra-short probe pulse experiences the EO effect induced by the THz pulse in the EO crystal. This EO effect, which is proportional to the electric field intensity of the THz wave, reflects the time varying information of the THz pulse across the diameter of the pulse-front tilted probe pulse. Thus, by detecting the probe pulse with a detector array, temporal information of the THz pulse is acquired from a single THz pulse.

In Ref. 8, we used an SF10 prism as a dispersing element. The tilt angle of the probe pulse front was 4.8°, and the time window, which is the full range of the measured time width, was 2.6 ps. These results demonstrate the basic principle of the technique, however, they are not suitable for spectroscopy because of the narrow time window. A time window of 2.6 ps is equivalent to a spectral resolution of 0.38 THz according to the sampling theorem. To apply

#144043 - $15.00 USD Received 11 Mar 2011; revised 25 Apr 2011; accepted 25 Apr 2011; published 25 May 2011

this technique to spectroscopy with performance equivalent to the conventional sampling method, the time window must be made about ten times wider. One way of achieving this is to increase the pulse-front tilt angle.

In this paper, we show single-shot THz spectroscopy using pulse-front tilting of a probe pulse by utilizing a transmission grating as a dispersing element to increase the tilt angle. We examined the distortion of the THz signal, which must be addressed in order to extend this single-shot technique to spectroscopy. The advantage of this technique compared with other single-shot techniques that also allow a large time window (e.g., spectral encoding [2], noncollinear geometry [4, 5], and use of echelons [6]) is its ability to achieve high temporal resolution and flexibility in adjusting the measuring time window. In our technique, since the probe pulse has femtosecond duration, high temporal resolution is maintained. In contrast to the noncollinear geometry, "cross-talk" does not occur even if a thick crystal is used, because the probe pulse is incident on a receiver crystal collinearly with the THz pulse. Furthermore, the time window can be arbitrarily adjusted because the tilt angle of the pulse front can be easily changed by suitable arrangement of a transmission grating and lens pair.

2. Experiment

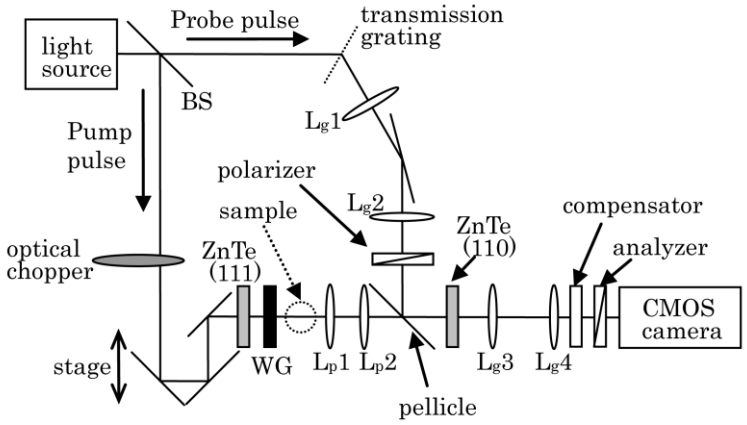

Fig. 2. Experimental setup of single-shot THz spectroscopy experiment. BS, beam splitter; WG, wire-grid polarizer; L_ps 1 and 2, plastic lens; L_gs 1-4, glass lens.

Figure 2 shows a diagram of the experimental setup, which was based on a THz real-time imaging system [11]. The light source was a Ti:sapphire laser based on the chirped pulse amplification technique (Legend, Coherent Inc.), which provided laser pulses with a central wavelength of 800 nm, a pulse duration of 50 fs, a pulse energy of 2.5 mJ, and a repetition rate of 1 kHz. Each laser pulse was split into pump and probe pulses at a beam splitter (BS). The pump pulse generated a THz pulse by optical rectification in a 1 mm-thick ZnTe (111) crystal. After passing through the sample, the THz pulse passed through two plastic lenses (L_ps 1 and 2 in Fig. 2) provided to relay an image of the sample position to the position of the THz receiver crystal. The THz receiver was a 1 mm-thick ZnTe (110) crystal.

The pulse front of the probe pulse was tilted by a transmission grating. Compared with a reflection grating, a transmission grating has some advantages: it is easy to utilize a Littrow-grating mount, and the optics setup is highly flexible because the diffracted laser pulse passes behind the grating. The tilt angle γ_0 of the pulse front of a laser pulse with central wavelength λ given by dispersive elements that provide angular dispersion $d\phi/d\lambda$ is expressed as [12]:

$$\tan\gamma_0 = -\lambda\frac{d\phi}{d\lambda}. \quad (1)$$

#144043 - $15.00 USD Received 11 Mar 2011; revised 25 Apr 2011; accepted 25 Apr 2011; published 25 May 2011

The angular dispersion $d\phi/d\lambda$ is calculated by differentiating the expression relating the incident angle and the diffraction angle of the grating.

After passing through the transmission grating, the probe pulse was imaged onto the receiver EO crystal by a first glass lens pair (L_gs 1 and 2). If the magnification of the first glass lens pair is M, the tilt angle γ of the probe pulse front on the EO crystal is expressed as:

$$\tan\gamma = \frac{1}{M}\tan\gamma_0. \tag{2}$$

We used a transmission grating with a groove density of 1250 grooves/mm and a first glass lens pair with a magnification, M, of 1.2. The pulse-front tilt angle of the probe pulse on the grating and on the EO crystal obtained from the above equations were 49.11° and 42.73°, respectively. The time window T is expressed as [8]:

$$T = \frac{\sigma\tan\gamma_0}{c}, \tag{3}$$

where c is the speed of light, and σ is the effective beam diameter of the probe pulse at the EO crystal. We used expansion optics as a second glass lens pair (L_gs 3 and 4) to suppress the influence of the laser beam's intensity distribution, which causes signal distortion, as described below (Sec. 3-2). By using the expansion optics, the beam diameter of the probe pulse became bigger than the probe pulse detector size. Therefore, the effective probe beam diameter σ became smaller than the original. σ was 8 mm, and so the estimated time window T for the measurement was 24.6 ps.

A compensator was set in front of the detector array to obtain the optimal bias position for the large modulation depth near the zero optical bias point [13], i.e., the zero optical transmission point. The detector for the probe pulse was an Intelligent Vision Sensor (IVS, C8201-05, Hamamatsu), a high-speed complementary metal oxide semiconductor camera that can acquire images of 512 by 512 pixels at 250 frames/s, and at 1000 frames/s for a limited set of pixels. We set the measuring range to 512 by 112 pixels at 1000 frame/s. The pump pulse was chopped at 500 Hz by an optical chopper to acquire a THz image based on dynamic subtraction [11, 14, 15]. Under the above experimental conditions, the time resolution was 0.048 ps/pixel, the Nyquist frequency was 10.4 THz, and the spectral resolution was 0.04 THz.

3. Results and discussions

In this section, we show the results of our single-shot measurement technique, and we discuss its effectiveness. We carried out spectroscopy of lactose using our single-shot measurement technique and a conventional sampling method and compared the results. The lactose was mixed with the same amount of polyethylene and shaped into a tablet by compression.

3.1 Spatiotemporal images obtained with single THz pulse

Figures 3(a) and 3(b) show the spatiotemporal images obtained with a single THz pulse. In the figure, (a) is the result obtained with no sample ("reference signal") and, (b) is the result obtained with a lactose tablet at the sample position of Fig. 2 ("sample signal"). The horizontal axis represents the time scale.

Stripes corresponding to the electric field vibration of the THz pulse appeared. These signals contained oscillations reflecting the main pulses, even in the reference signal. This was due to the influence of water vapor. We can eliminate this influence because it appeared in both the reference and sample signals. Ideally, however, we should carry out measurements under a nitrogen purge or in a vacuum for more precise observation.

#144043 - $15.00 USD Received 11 Mar 2011; revised 25 Apr 2011; accepted 25 Apr 2011; published 25 May 2011

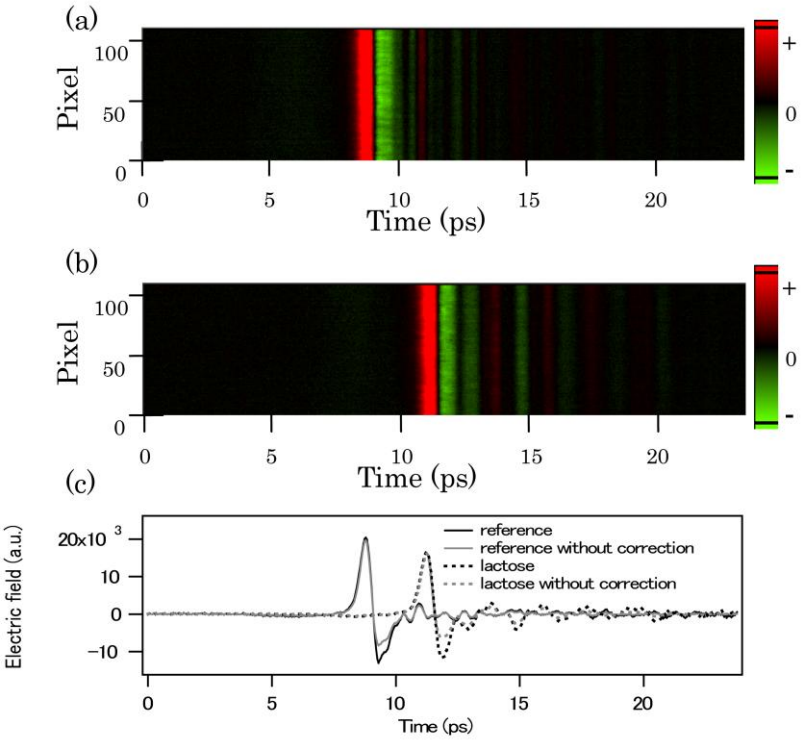

Fig. 3. (a), (b) Spatiotemporal image obtained by single THz pulse with (a) no sample, and (b) lactose tablet sample. (c) Temporal waveforms extracted from (a) (solid line) and (b) (broken line). Black line represents waveforms corrected for distortion and gray line represents uncorrected waveforms. Time-axis is in accord through (a), (b), and (c).

The time axis was calibrated by checking the relation between the displacement of the stage and a shift of the stripes. When we moved the stage 2400 μm, the stripes shifted 344 pixels. A stage displacement of 2400 μm corresponds to a time delay of 16 ps. Therefore, the calibration value for the time axis was 0.0465 ps/pixel. The time window was 23.8 ps, which agrees with the estimated value. Furthermore, the stripes shifted linearly with the stage displacement, indicating that the pixels were at regular intervals on the time axis.

3.2 Elimination of distortion

To use the acquired temporal waveform for spectroscopy, we have to eliminate the influence of two kinds of distortion.

The first is the influence of the intensity distribution along the beam cross-section. The intensity of a femtosecond laser pulse is lower at both ends of the beam cross-section than at the central part because of the beam's Gaussian profile. For this reason, the THz signal also became low at both ends of the time scale. We suppressed this effect by expanding the probe beam so that it was larger than the detector and used the center part of the laser beam as the probe beam; however, some differences remained. To remove this distortion completely, we acquired the beam profile of the THz beam with the following procedure: We swept the stage so that a stripe moved from one end to the other end of the measurement window (Fig. 3(a)). During this process, we recorded the maximum value at all pixels. Figure 4 shows the acquired THz beam profile. This profile included effects such as the probe and THz beam profiles, the non-uniformity of the ZnTe crystal, and the signal nonlinearity due to the crossed-Nicols arrangement employed (described below).

#144043 - $15.00 USD Received 11 Mar 2011; revised 25 Apr 2011; accepted 25 Apr 2011; published 25 May 2011

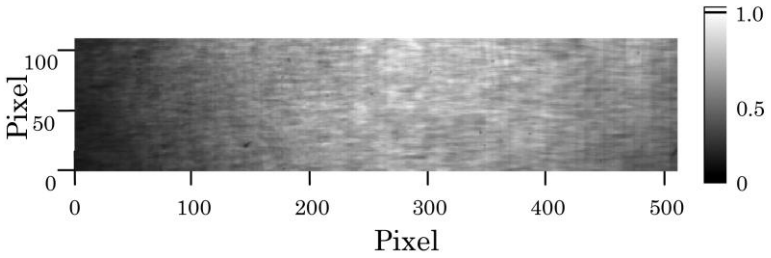

Fig. 4. Acquired THz beam profile. Intensity is normalized by peak value.

The second distortion is the nonlinearity of the measured signal due to the crossed-Nicols arrangement. In a crossed-Nicols arrangement, the output signal has a quadratic dependence on the THz wave amplitude [16]. The compensator was placed in front of the polarizer and was set at the optimal bias point to increase the modulation depth, not at the bias point used for linear detection, so that the optical bias remained near the zero transmission point (zero bias) [13]. This nonlinearity was evaluated by investigating the change of the output signal when changing the intensity of the THz pulse [17]. In doing so, it was necessary to measure not only the positive electric field but also the negative electric field. We made a calibration table to correct the nonlinearity using a ZnTe (111) crystal and a wire-grid (WG) polarizer. The ZnTe (111) crystal, when used as a THz emitter crystal, has the following unique features. The polarization direction of the generated THz pulse from the ZnTe (111) crystal rotates at a rate three times greater than the rotation of the polarization direction of the optical pump pulse. That is, when we rotate the ZnTe (111) crystal by 10° and the polarization of the optical pump pulse is linear, the polarization direction of the THz pulse will rotate by 30°, maintaining the linear polarization. In addition, the energy of the generated THz pulse, i.e., the conversion efficiency, is constant for all polarization directions [18]. Therefore, the amplitude and the positive/negative values of the electric field of a THz pulse can be controlled by arranging the fixed WG polarizer behind the ZnTe (111) crystal and rotating the ZnTe crystal. Calibration tables have to be made for all pixels because of the non-uniformity of the ZnTe crystal (Fig. 4). Therefore, we acquired a beam profile of a THz pulse like that shown in Fig. 4 every 2° of rotation of the ZnTe (111) crystal. Figure 5 shows the measured nonlinearity of one pixel. A fitted curve is also displayed (red line). The calibration table for the second type of distortion was made by dividing the linear line (blue line) by the fitted curve.

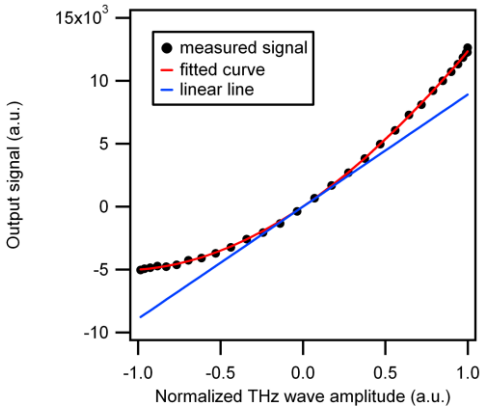

Fig. 5. Example of measured nonlinearity of our optical system. Dots show measured signal. Red line shows fitted curve. Linear line is also displayed (blue line).

The following describes the correction procedures used for the results shown in Figs. 3(a) and 3(b) using the beam profile of the THz pulse and a calibration table for correcting the

#144043 - $15.00 USD Received 11 Mar 2011; revised 25 Apr 2011; accepted 25 Apr 2011; published 25 May 2011

nonlinearity originating from the crossed-Nicols arrangement. First, the nonlinearity in Figs. 3(a) and 3(b) was corrected using the calibration table. Second, the beam profile of the THz pulse (Fig. 4) was also corrected for the nonlinearity using the calibration table. Finally, the influence of the intensity distribution along the beam cross-section was eliminated by dividing the calibrated results in Figs. 3(a) and 3(b) by the calibrated beam profile of the THz pulse. Figure 3(c) shows the temporal waveforms extracted from Figs. 3(a) and 3(b). The black line is a corrected signal, and the gray line is the raw data. The solid line was extracted from Fig. 3(a), and the broken line was extracted from Fig. 3(b).

3.3 THz spectrum and absorption coefficient of lactose tablets

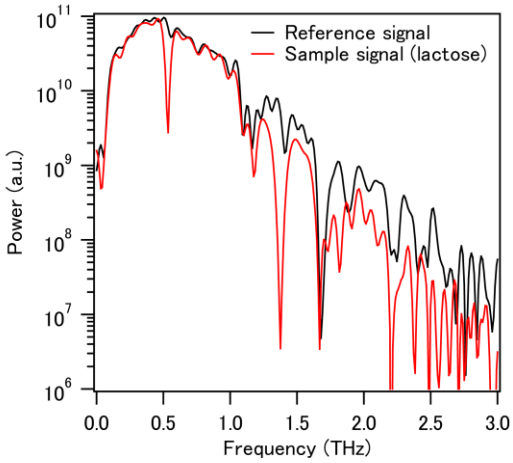

Fig. 6. Power spectra of reference and sample signals obtained with single THz pulse.

Figure 6 shows the power spectrum obtained by fast Fourier transformation (FFT) of the corrected temporal waveform shown in Fig. 3(c) (solid black line). The spectral bandwidth, which is limited by the properties of the 1 mm-thick ZnTe crystal [19], was ~2.5 THz. The peak frequency was 0.5 THz. The maximum dynamic range, defined as the ratio of the maximum THz signal to the noise floor, was ~34 dB.

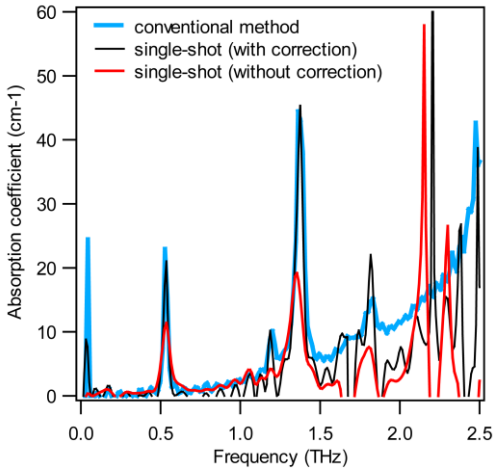

Fig. 7. Absorption spectra of lactose tablet. Results obtained by conventional sampling measurement and single-shot measurement (with and without correction) are shown for comparison.

#144043 - $15.00 USD Received 11 Mar 2011; revised 25 Apr 2011; accepted 25 Apr 2011; published 25 May 2011

Figure 7 shows the absorption spectrum of a lactose tablet. The black line was obtained using a corrected signal, and the red line was obtained using raw data. To evaluate these results, we compared them with the result obtained from the conventional sampling measurement, in which photo-conductive dipole antennas as a THz emitter and receiver. The bandwidth was ~4 THz, and the dynamic range was ~70 dB. The result of the conventional sampling measurement is shown in Fig. 7 as a blue line. The characteristic absorption peaks of 0.53 and 1.37 THz in the results of the single-shot measurement with the correction and the conventional method are quantitatively equivalent. The absorption spectra did not agree in the region higher than 1.5 THz. The cause is probably the insufficient signal-to-noise ratio at higher frequencies.

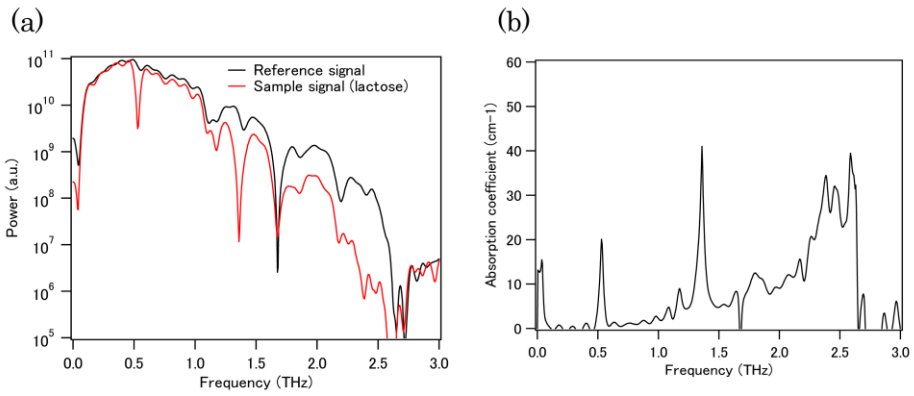

Fig. 8. Spectra obtained with 50 averaged terahertz pulses (10 fps). (a) Power spectrum and (b) absorption spectrum of lactose tablet.

Figure 8 shows the spectra obtained with an average of 50 THz pulses. They were acquired in real time (10 fps). Figure 8(a) shows power spectra of the reference and sample signals. Figure 8(b) shows absorption spectra of the lactose tablet. The signal-to-noise ratio improved, and a scattering background at higher frequencies up to 2.5 THz appeared, which agrees well with the blue line of Fig. 7.

4. Conclusions

We demonstrated THz single-shot spectroscopy using a tilted pulse front. Use of a transmission grating as the dispersive element extended the measuring time window to 23.8 ps, which is about ten times greater than that achievable with prisms. To demonstrate the effectiveness of single-shot measurement using a tilted pulse front, we measured the spectrum of lactose. The results obtained using the single-shot technique and the conventional sampling method were in good agreement quantitatively for the characteristic absorption peaks of lactose at 0.53 and 1.37 THz.

Acknowledgments

The authors thank A. Hiruma, K. Yamamoto, and Y. Suzuki for their encouragement and K. Shibayama and M. Fujimoto for their helpful discussions.

#144043 - $15.00 USD Received 11 Mar 2011; revised 25 Apr 2011; accepted 25 Apr 2011; published 25 May 2011